ELSEVIER

Journal of Chromatography A, 746 (1996) 169–183

JOURNAL OF CHROMATOGRAPHY A

Characterization of protein adsorption by composite silica–polyacrylamide gel anion exchangers I. Equilibrium and mass transfer in agitated contactors

M. Aurora Fernandez[1], Giorgio Carta*

Center for Bioprocess Development, Department of Chemical Engineering, University of Virginia, Charlottesville, VA 22903-2442, USA

Received 1 December 1995; revised 10 April 1996; accepted 11 April 1996

Abstract

The uptake of proteins by composite porous silica–polyacrylamide gel ion exchangers known under the trade name HyperD, is investigated. These ion exchangers are found to have an exceptionally high static adsorption capacity, greater than about 200 mg/cm^3, and a rapid uptake kinetics. Being mechanically quite strong, they are suitable for chromatography applications at elevated mobile phase flow-rates. The uptake equilibrium of proteins by these ion exchangers is obtained experimentally and is found to follow the mass action law. Thus, reversible adsorption and desorption of proteins is obtained by varying the solution ionic strength. Batch mass transfer rates in an agitated contactor under favorable uptake conditions are also obtained. The uptake kinetics is controlled by the fluid phase mass transfer resistance for low protein concentrations, and by the intraparticle mass transfer resistance at high protein concentrations. In the latter case, the uptake is quite rapid and nearly complete saturation of particles 49–76 μm in diameter can be obtained in 5 to 10 min. The parameters of a model describing the batch uptake kinetics in these ion exchangers are obtained by comparing experimental results with model predictions.

Keywords: Mass transfer; Ion exchangers; Stationary phases, LC; Preparative chromatography; Proteins; Albumin; Ovalbumin; Lactalbumin

1. Introduction

The optimized design of stationary phases suitable for preparative chromatography of biological macromolecules frequently requires that a compromise be struck among capacity, adsorption kinetics, and flow characteristics. Each of these factors affects the performance of a given stationary phase and maximizing each independently is a constant challenge for media manufacturers. Biological macromolecules have low diffusivity and this limits to a great extent the rate of intraparticle mass transfer.

Both rigid porous matrices and soft, gel-type media are used extensively in protein chromatography. Stationary phases comprising porous rigid matrixes, such as silica or crosslinked polystyrene, must have large pores to minimize diffusive hindrance. This may limit the available surface area and, thus, the uptake capacity. Being structurally strong, however, such materials can tolerate large pressure

*Corresponding author

[1]Current address: Departamento de Ingegneria Quimica, Universidad de Oviedo, Spain.

0021-9673/96/$15.00
PII S0021-9673(96)00337-8

gradients with little or no compression. Hence, small particles can be used to reduce mass transfer resistance while operating at high flow-rates. On the other hand, "soft", gel-type stationary phases, such as polyacrylamide, cross-linked dextran, agarose, or cellulose, can exhibit a large adsorption capacity since a very high concentration of functional groups is achievable. However, they are generally quite compressible and, thus, they are only useful over a limited range of mobile phase flow-rates. Moreover, these materials can be susceptible to significant volume changes occurring when the mobile phase composition is changed.

A number of approaches have been introduced in the past to circumvent low diffusion rates in stationary phases for protein chromatography and increase the speed of separation. The use of pellicular particles, comprising a thin retentive layer held on the surface of a non-porous support, has been suggested [1,2]. Such stationary phases eliminate intraparticle mass transfer limitations, but they have only a very low capacity and thus they are useful essentially only in analytical applications. A second approach is the use of porous stationary phases which are permeable to fluid flow [3,4]. Such stationary phases can have a bimodal pore structure including smaller pores that provide a large fraction of the adsorption capacity and large connected pores that allow convective fluid transport. Under appropriate conditions in packed columns, intraparticle convection enhances the rate of mass transfer of slowly diffusing solutes increasing the speed of separation [5–9]. A third approach which has been suggested is the use of composite stationary phases that combine the desirable characteristics of rigid porous media with those of soft-gel matrices. These stationary phases comprise a rigid skeleton that provides mechanical strength and a soft gel for the interaction with the solutes to be separated [10]. Examples of such materials include porous silica–dextran composites [11], Kieselguhr–agarose composites [12], and polyhydroxylethyl methacrylate (HEMA)–dextran composites [13]. Composite media can be designed to have a large adsorption capacity realized through the high density of functional groups which is achievable with gels. At the same time, elevated mobile phase flow-rates can be tolerated because of the structural strength of the rigid support.

Recently, porous silica–polyacrylamide composite stationary phases, known under the trade name HyperD, have been introduced for ion-exchange chromatography of proteins [10]. A version of these materials, which is studied in this work, comprises a very low surface area and high porosity polystyrene–silica matrix whose pores are filled with a functionalized polyacrylamide gel. The result of this association is a high capacity stationary phase that can be used at high flow-rates of the mobile phase in a chromatography column. For one such medium Boschetti [10] has reported an adsorption capacity for bovine serum albumin (BSA) of 125 mg/cm^3 with an efficiency of utilization of the functional groups of 0.85 mg of protein per μequiv. of ionogenic groups. Based on the high dynamic capacity exhibited by HyperD media at relatively high flow-rates, Boschetti concluded that the hydrogel filling of these materials provides access to the active sites by rapid diffusion mechanisms. The chromatographic performance of materials of this type has also recently been discussed by Horvath et al. [14]. Other authors [15] have shown that the HyperD media is stable in oxidizing agents, such as peracetic acid, which can be used to obtain a very rapid and effective in-situ sanitization, making these stationary phases attractive for preparative applications.

In this work, we have determined experimentally the equilibrium uptake of representative proteins by Q-HyperD anion-exchange media as well as mass transfer rates in a stirred, finite bath, batch contactor. The experimental results are expressed in terms of equilibrium and kinetic models to obtain values of characteristic parameters useful for predicting the behavior of these stationary phases in chromatographic applications. Mass transfer rates in packed columns and dynamic capacity data are given in Part II of this paper, along with a model to predict the breakthrough behavior.

2. Experimental

2.1. Materials

HyperD stationary phases (BioSepra, Marlborough, MA, USA) were used in this work. These

materials consist of macroporous polystyrene–silica particles whose pores are filled with a functionalized polyacrylamide hydrogel. The Q-HyperD media contains a quaternary ammonium ion functionality and, thus, is a strong-base anion exchanger. Some details on the preparation of matrices of this type are given by Girot and Boschetti [16].

Two grades of Q-HyperD media were obtained from BioSepra, Q-HyperD-F (Lot No. 3259) and Q-HyperD-M (Lot No. 3186). These two grades differ only in their particle size. Each sample was pretreated with a 1 *M* NaCl solution and rinsed with a 50 m*M* Tris–HCl aqueous buffer at pH 8.6. Excess buffer was then removed from the hydrated media by centrifugation in a centrifuge tube equipped with a glass frit before storing the samples in sealed containers. The total water content of each media sample pretreated in this manner was determined from the mass loss on drying in an oven at 110°C. It varied between 55 and 58% (w/w) depending on the extent of centrifugation.

The particle density of hydrated HyperD particles was estimated to be 1.424 g/cm^3. This value was obtained using the porosity value of 0.65 of the dry matrix used to prepare the HyperD media [17] and by assuming a density of 1.0 g/cm^3 for the hydrogel that fills the pores of the particles in their hydrated state. A skeletal density of 2.21 g/cm^3 was assumed for the silica backbone of the support matrix. The estimated particle density agrees with the manufacturer estimate of specific gravity between 1.3 and 1.5 [18].

We also determined the particle size distribution of each of the HyperD by taking microphotographs of hydrated particles in aqueous suspension at 100× magnification with a Bausch and Lomb (Rochester, NY, USA) Balplan microscope. The preponderant particle shape was spherical in each case, although each sample contained many irregular particles. Thus, for a consistent determination, for each particle in a micrograph section containing at least 120 particles, we obtained an approximate equivalent spherical size with the aid of a calibrated template. The corresponding distribution of particle sizes is given in Fig. 1a and b on a volume fraction basis. The volume-average particle diameters were 49 μm and 76 μm respectively for the F and M grades of Q-HyperD.

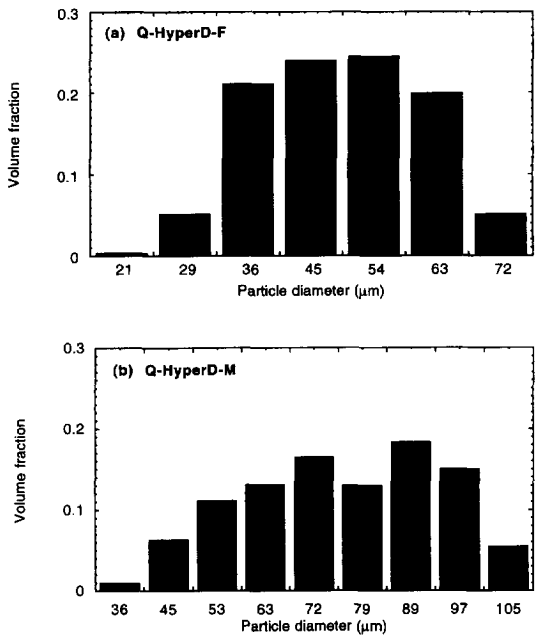

Fig. 1. Particle size distribution of Q-HyperD media. (a) Q-HyperD-F, Lot. 3259, (b) Q-HyperD-M, Lot. 3186.

Three different proteins were used as model compounds: BSA (M_r~65 000, pI~4.9), ovalbumin (OVA, M_r~45 000, pI~4.6), and α-lactalbumin from bovine milk (LACT, M_r~16 000, pI~5). Purified preparations of these proteins were obtained from Sigma (St. Louis, MO, USA). Proteins solution were prepared by dissolving these samples in 50 m*M* Tris–HCl aqueous buffers at pH 8.5–8.6. At this pH, each protein is strongly negatively charged and is thus suitable for ion-exchange with Q-HyperD. The concentration of each protein in solution was obtained spectrophotometrically at 280 nm using a Beckman (Fullerton, CA, USA) Model DU50 spectrophotometer.

2.2. Equilibrium experiments

The static equilibrium uptake capacity of Q-HyperD media was determined for each protein from batch experiments. In these experiments, solutions containing initial known concentrations of protein (10 cm^3) were contacted with a known amount of HyperD media (0.025 cm^3) in sealed test tubes, rotated end to end in a laboratory rotator at about 60

rpm. After attainment of equilibrium (which was demonstrated by the fact that there was no further variation in the sample), the supernatant was sampled to determine the residual protein concentration in each tube by spectrophotometric analysis. The amount of protein adsorbed was then obtained from the material balance

$$q = \frac{V}{V_M}(C_0 - C) \quad (1)$$

where q is the amount of protein adsorbed per unit volume of media, V is the volume of solution, V_M the volume of media, and C_0 and C are respectively the initial and equilibrium protein concentration in solution. Since the total water content of the media samples used was somewhat variable, in order to standardize conditions, the results were expressed in terms of the volume of hydrated particles. This was obtained from the dry mass of each media sample determined as described above together with the estimated apparent density of the dry particles. All experiments were carried out at room temperature (23±2°C).

2.3. Batch kinetics experiments

The amount of protein taken up as a function of time by the HyperD media in an agitated contactor was obtained for each of the test proteins and particle size grades. The apparatus used for these determinations is similar to the one used by Grzegorczyk and Carta [19] and comprises a glass vessel (5 cm in diameter and 7 cm long) with a slightly conical, upwardly pointing bottom. This vessel is equipped with a PTFE-coated, magnetically driven impeller with 4-cm flat blades. The impeller shaft rests between a recess in the vessel lid at one end and the conical bottom of the vessel at the other. This arrangement prevented destruction of the media by grinding. Q-HyperD media samples were fully suspended in the vessel by agitation at approximately 300 rpm. The protein concentration in solution was monitored by continuously recirculating a small stream through a spectrophotometer (Bausch and Lomb, Spectronic Model 601) equipped with a low-volume quartz flow cell. This stream was drawn through a 10-μm stainless-steel frit (Upchurch Scientific, Oak Harbor, WA, USA, Model A302) with a Cole–Parmer (Niles, IL, USA) peristaltic pump, passed through the flow cell and returned to the vessel. The total response time of the circulation loop and detection system was estimated to be about 5 s by observing the absorbance readings in response to a step change in concentration in the vessel in the absence of stationary phase. The residence time in the loop, estimated from the tubing and flow cell volumes and the pump flow-rate, was actually smaller than 5 s.

Transient uptake experiments with BSA were performed either by quickly introducing a media sample in a volume of solution already loaded in the vessel, or by injecting a bolus of BSA into a volume of buffer in which the media sample was already suspended. The two techniques yielded essentially the same result, except for very short times, where the former technique appeared to yield more consistent results. This technique was thus used for experiments with ovalbumin and lactalbumin. In each case, 100 cm^3 solutions containing different initial protein concentrations in the range 0.1–2 mg/cm^3 were contacted with 0.25 cm^3 samples of Q-HyperD. The exact volume of particles introduced in the vessel was determined as before using the known mass of the sample, its water content, and the estimated apparent particle density.

The spectrophotometer digital absorbance signals were collected with a microcomputer (AT&T, New York, NY, Model PC6300) and converted to concentration with calibration curves. As in the case of batch equilibrium experiments, the amount of protein taken up by the media at each time was obtained from the material balance, Eq. (1). The experiments were all carried out at room temperature.

3. Results and analysis

3.1. Uptake equilibrium

The uptake equilibrium of BSA by Q-HyperD-F and -M is shown in Fig. 2 for 50 m*M* Tris–HCl buffer solutions containing different NaCl concentrations. The uptake of ovalbumin and α-lactalbumin by Q-HyperD-M in 50 m*M* Tris–HCl buffer is given in Fig. 3 and Fig. 4. The uptake of each of the proteins studied is clearly very favorable for these

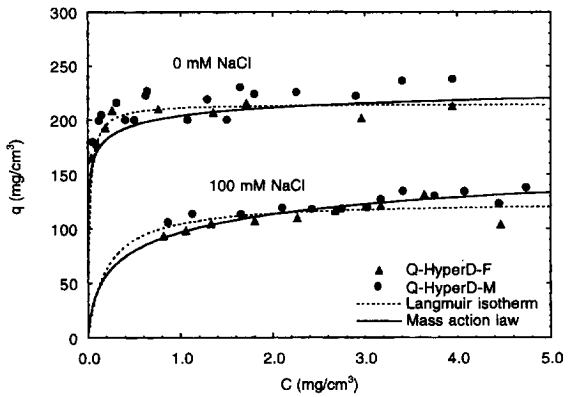

Fig. 2. Equilibrium uptake of BSA by Q-HyperD media at different NaCl concentrations in a 50 m*M* Tris–HCl buffer at pH 8.6. Lines are calculated from the Langmuir isotherm (Eq. 2) and from the mass action law isotherm (MA, Eq. 3b) using the parameters in Table 1.

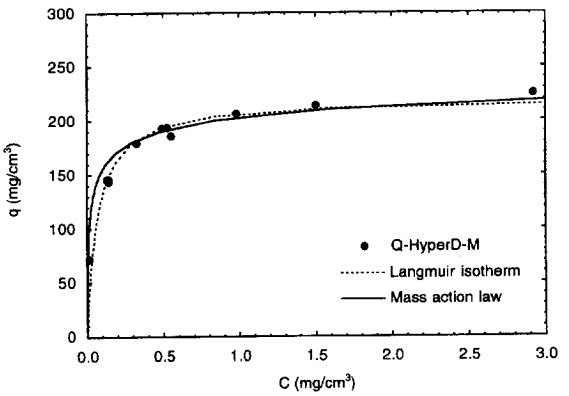

Fig. 4. Equilibrium uptake of α-lactalbumin by Q-HyperD-M in a 50 m*M* Tris–HCl buffer at pH 8.6. Lines are calculated from the Langmuir isotherm (Eq. 2) and from the mass action law isotherm (MA, Eq. 3b) using the parameters in Table 1.

conditions. As is shown by the BSA data, however, the uptake is depressed by the addition of salt. We found that at salt concentrations greater than about 300 m*M* there was no retention of BSA by Q-HyperD media. We also found that essentially all of the BSA taken up in the absence of salt could be desorbed by adding 500 m*M* NaCl to the solution. The two grades of Q-HyperD yielded essentially the same uptake capacity for BSA at both high and low salt concentrations.

The uptake capacity of these ion exchangers, leveling off at about 200 mg/cm^3, is indeed quite high. If the silica matrix is considered inert, this uptake capacity can be translated into about 300 mg of protein per cm^3 of gel-filled pores. Such a high capacity is not uncommon in soft gel media [10], but is rarely found in rigid porous matrices that rely on surface area for their capacity.

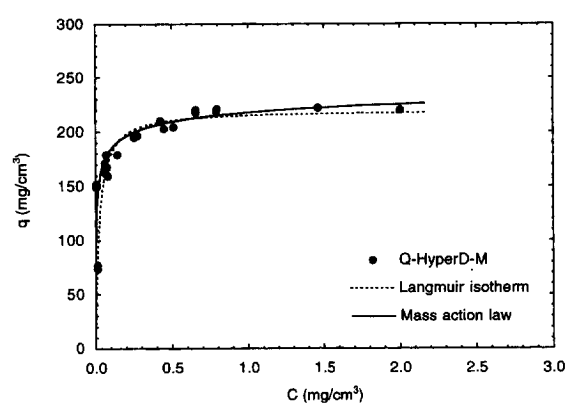

Fig. 3. Equilibrium uptake of ovalbumin by Q-HyperD-M in a 50 m*M* Tris–HCl buffer at pH 8.6. Lines are calculated from the Langmuir isotherm (Eq. 2) and from the mass action law isotherm (MA, Eq. 3b) using the parameters in Table 1.

Two models were used to fit the experimental uptake isotherms. The first one is the Langmuir isotherm which is expressed by

$$q = \frac{q_m b C}{1 + bC} \tag{2}$$

where q_m is the maximum adsorption capacity and b is an affinity coefficient. Because the uptake of proteins by ion exchangers involves a heterovalent interaction with the media functionality, the physical assumptions underlying the theoretical derivation of the Langmuir isotherm are violated [20]. Thus, Eq. (2) is generally unable to fit data at different salt concentrations unless different values of both q_m and b are used for each condition. Nevertheless, in spite of its shortcomings such a model has been used successfully by several authors [21–23] to describe the uptake of proteins by anion and cation exchangers in a purely empirical way.

The second model considered in this work is one based on the mass action law for the heterovalent exchange of protein and salt counterions. According to this formalism the equilibrium uptake of a protein is viewed as the result of the stoichiometric exchange of protein and salt counterions. For a univalent salt,

I, and a protein, P, with an effective charge n, this is expressed by [24,25]

$$nRI + P \rightleftharpoons R_nP + nI \tag{3}$$

with equilibrium constant

$$K = \frac{[R_nP][I]^n}{[RI]^n[P]} = \frac{qC_I^n}{q_I^nC} \tag{3a}$$

where R represents the functional groups in the ion exchanger. These have a fixed concentration $q_R = nq + q_I$. The following isotherm expression is obtained relating the concentration of protein in solution, C, to the concentration of protein in the ion exchanger, q, and to the counterion concentration in solution, C_I

$$C = \frac{qC_I^n}{Kn^n(q_n - q)^n} \tag{3b}$$

where $q_n = q_R/n$.

The two models described above, although not rigorous, could fit the experimental data for the uptake of proteins by Q-HyperD media approximately equally well within the apparent scatter of the results as is shown in Figs. 2–4. The Langmuir isotherm parameter were obtained at each salt concentration, while for the mass action law model, only one set of parameters was found to fit the data accurately at both salt concentrations used for BSA (0 and 100 mM). Thus, an advantage of this model appears to be the fact that the effect of the counterion concentration can be predicted without a need for additional parameters. In fitting the mass action law model for the uptake of ovalbumin and lactalbumin, since data were only available in the absence of added salt ($C_I = [Cl^-] = 50$ mM), q_n was assumed to have the same value as that found for BSA, while n and K were determined from a data fit. It should be noted that it could also be possible to fit the ovalbumin and lactalbumin data using the same value of q_R (the total ion-exchange capacity of the media) as that found for BSA. Using the same q_n value proved however satisfactory, since the effect of salt concentration is not considered for ovalbumin and lactalbumin. The fitted parameters values are summarized in Table 1. Values of the equilibrium constant K are given for the practical units of mmol/mg of protein for use in 3b with q and C expressed in mg/cm^3 and C_I in mmol/cm^3. The values of the dimensionless equilibrium constant are found by multiplying the K values in Table 1 by the molecular mass of each protein to the power n. The corresponding values of K are $2.8 \cdot 10^7$, $4.4 \cdot 10^6$, and $1.6 \cdot 10^4$ for BSA, ovalbumin, and α-lactalbumin, respectively.

Other more complicated models taking into account steric interactions could be considered as perhaps more realistic approximations. Brooks and Cramer [26], for example, have shown that a model that takes into account the partial shielding of functional groups on the support can provide a more accurate representation of protein equilibrium uptake by ion exchangers. Although potentially quite useful, we did not make use of this model in fitting the data since the range of salt concentrations considered was not sufficient to provide a statistically meaningful evaluation of the added parameter that appears in this model.

3.2. Uptake kinetics

Mass transfer in a gel-type ion exchanger is potentially affected by two resistances in series: the external film resistance and the intraparticle mass transfer resistance. The following set of conservation equations and boundary conditions can be written to relate these two transport resistances to the experimental batch uptake kinetics.

Table 1
Equilibrium parameters for adsorption on Q-HyperD media in a 50 mM Tris–HCl buffer at pH 8.6

Protein	[NaCl] (mM)	q_m (mg/cm^3)	b (cm^3/mg)	q_n (mg/cm^3)	n	K (mmol/mg)^n
BSA	0	215	50	270	5.35	$5.0 \cdot 10^{-19}$
BSA	100	125	5.0	270	5.35	$5.0 \cdot 10^{-19}$
OVA	0	220	45	270	4.30	$4.3 \cdot 10^{-14}$
LACT	0	220	15	270	3.80	$1.7 \cdot 10^{-12}$

For the particles:

$$\frac{\partial q}{\partial t} = \frac{D_s}{r^2}\frac{\partial}{\partial r}\left(r^2\frac{\partial q}{\partial r}\right) \tag{4}$$

$$r = 0, \frac{\partial q}{\partial r} = 0 \tag{4a}$$

$$r = R_p, D_s\frac{\partial q}{\partial r} = k_f(C - C_i) \tag{4b}$$

$$t = 0, q = 0 \tag{4c}$$

and for the solution:

$$\frac{dC}{dt} = -\frac{3k_f}{R_p}\frac{V_M}{V}(C - C_i) = -\frac{V_M}{V}\frac{d\bar{q}}{dt} \tag{5}$$

$$t = 0, C = C_0 \tag{5a}$$

where $\bar{q}$ is the average solute concentration in the particle. Equilibrium may be assumed to exist at the particle–fluid interface. Thus, using, for example, the mass action law equilibrium model, the interfacial concentrations $q_i = q(R_p)$ and C_i are related by

$$C_i = \frac{q_i C_I^n}{Kn^n(q_n - q_i)^n} \tag{6}$$

In these equations, R_p is the particle radius, D_s is the intraparticle protein diffusivity, and k_f is the external film mass transfer coefficient at the particle–fluid interface. The latter accounts for the mass transfer resistance in the hydrodynamic boundary layer that surrounds the particle.

Eq. (4), with its associated boundary conditions, is based on the assumption that the driving force for diffusion in the particle is the total protein concentration. Assuming that protein diffusion occurs only through the gel-filled pores, the actual gel-diffusivity is related to D_s through the porosity and tortuosity of the unfilled support matrix. A similar assumption regarding the driving force for intraparticle mass transfer has previously been used by Tsou and Graham [21] and by Graham et al. [27] to describe the uptake of proteins in dextran-based ion exchangers. These authors formulated their model using a "linear driving force approximation" to describe intraparticle mass transfer in terms of homogeneous diffusion and a film mass transfer coefficient to describe mass transfer outside the particle. More complicated models, accounting for parallel surface and pore diffusion of proteins in ion exchangers have also been considered by other authors. Bloomingburg and Carta [23], for example, found that the transient batch uptake of hemoglobin by S-Sepharose could only be described by assuming that diffusion of bound protein occurs in parallel with pore diffusion of unbound protein. A similar conclusion was reached recently by Yoshida et al. [28] for the transient uptake of BSA by a strong-base chitosan ion exchanger.

The relative importance of external and intraparticle mass transfer resistances is strongly dependent on the solution composition. The uptake of proteins by Q-HyperD at low salt concentrations is extremely favorable, as is shown by the nearly rectangular shape of the isotherms depicted in Figs. 2–4. Thus, as a practical matter, the protein concentration in the stationary phase is nearly constant and essentially independent of the protein solution concentration. For these conditions, a simple criterion is available to determine the controlling resistance in terms of the magnitude of the dimensionless group [29]

$$\delta = \frac{1}{5}\frac{k_f R_p}{D_s}\frac{C_0}{q_0} \tag{7}$$

where q_0 is the saturation capacity of the adsorbent. When δ is small compared to unity, the external film resistance is dominant. In this case, the protein concentration at the particle surface is negligibly small and the uptake rate is proportional to the bulk fluid phase solution concentration. Conversely, when δ is large compared to unity, the intraparticle mass transfer resistance is dominant. For these conditions, when the uptake isotherm is highly favorable, the protein concentration at the particle surface is nearly constant and equal to the saturation capacity. The uptake rate is then essentially independent of the bulk fluid phase concentration. Clearly, this criterion is not rigorous as it is derived simply by comparing the time scales of the two transport processes considered independent of each other. Thus, for example, the criterion is not valid for very short times, when the external film resistance is always dominant [29]. It is also not valid for very long times, when the adsorbent is nearly saturated and intraparticle mass transfer becomes very slow. Nevertheless, this criterion allows one to simplify the

determination of D_s and k_f by considering experimental conditions leading to the two asymptotic cases of external film and intraparticle mass transfer control. This can be attained in the stirred batch experiments by operating with very low and very high protein concentrations. The limiting solutions are found as follows. Under external film mass transfer control, $C_i \sim 0$. Thus, Eq. (5) can be integrated directly yielding the following result for the protein concentration in solution, C, and for the average protein concentration in the adsorbent, $\bar{q}$,

$$\frac{C}{C_0} = \exp\left(-\frac{3k_f}{R_p}\frac{V_M}{V}t\right) \tag{8}$$

$$\bar{q} = \frac{VC_0}{V_M}\left[1 - \exp\left(-\frac{3k_f}{R_p}\frac{V_M}{V}t\right)\right] \tag{8a}$$

Under intraparticle mass transfer control, $q_i = q(R_p) \sim q_0$, and Eq. (4) can be integrated directly yielding the well known result [29]

$$\frac{\bar{q}}{q_0} = 1 - \frac{6}{\pi^2}\sum_{k=1}^{\infty}\frac{1}{k^2}\exp\left(-\frac{k^2\pi^2 D_s t}{R_p^2}\right) \tag{9}$$

A useful approximation of this series solution suitable for approximate numerical calculations, is given by Helfferich and Plesset [30] as

$$\frac{\bar{q}}{q_0} \sim \{1 - \exp\{\pi^2[-\tau + 0.960\tau^2 - 2.92\tau^3]\}\}^{1/2} \tag{10}$$

where $\tau = D_s t/R_p^2$.

Using the limiting solutions described above k_f and D_s can be determined independently by fitting 8a to transient uptake data obtained at a protein concentration sufficiently low that film resistance is dominant and by fitting Eq. (9) or Eq. (10) to transient data obtained at a concentration sufficiently high that intraparticle mass transfer is dominant. Of course, data at intermediate concentrations will not conform to either equation and will require that a full solution of the model (Eqs. (4–6)) be used to predict the results. It should be noted that a more general criterion to determine the controlling resistance which includes the effect of selectivity is given in [29]. The criterion used here is valid when the selectivity is very high as in the case of the low salt concentrations used experimentally in this work.

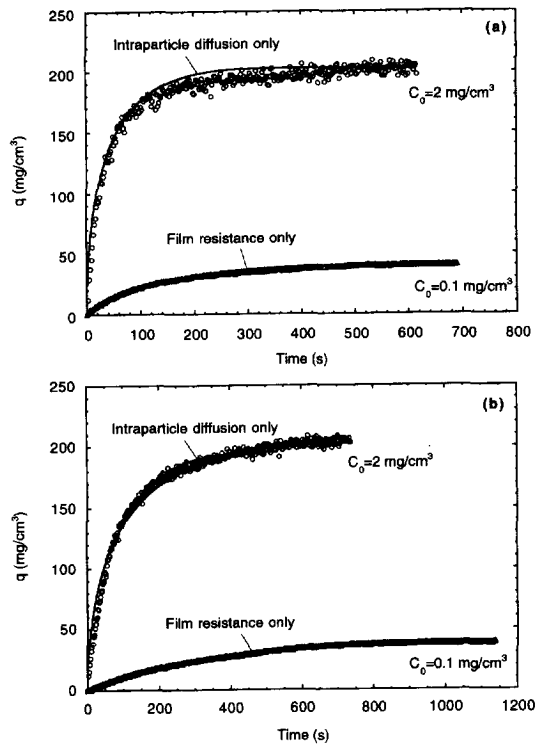

Fig. 5. Transient uptake of BSA by Q-HyperD media in an agitated contactor for (a) Q-HyperD-F and (b) Q-HyperD-M in a 50 m*M* Tris–HCl buffer at pH 8.6. Lines are calculated from Eq. (8a) for $C_0 = 0.1$ mg/cm^3 and from Eq. (10) for $C_0 = 2$ mg/cm^3.

Experimental data showing the amount of protein taken up as a function of time are given in Fig. 5 and Fig. 6 for the lowest and highest initial protein concentrations used. At the lowest concentrations, the amount of protein present in the vessel is insufficient to completely saturate the media sample. Thus, for these conditions, toward the end of the experiment the solution protein concentration acquired vanishingly small values. However, when an initial concentration of 2 mg/cm^3 was used, the amount absorbed equaled the saturation capacity previously determined in equilibrium experiments. For each of the proteins, Eqs. (8a) and (10) were used to fit the low and high concentration data shown in these figures. The resulting values of D_s and k_f are summarized in Table 2 and calculated lines are shown in the corresponding figures for BSA, ovalbumin and α-lactalbumin. Table 2 also gives the calculated Sherwood number ($Sh = d_p k_f/D$) using the

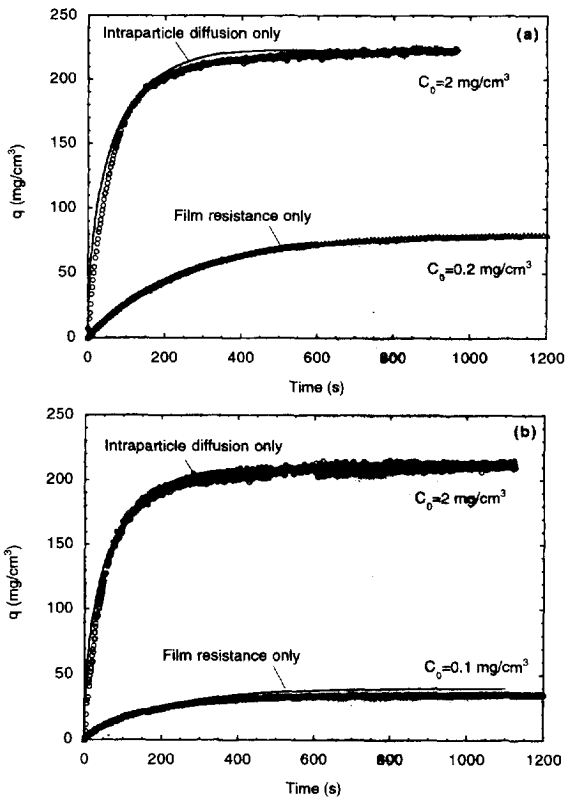

Fig. 6. Transient uptake of (a) ovalbumin and (b) α-lactalbumin by Q-HyperD-M in an agitated contactor in a 50 m*M* Tris–HCl buffer at pH 8.6. Lines are calculated from Eq. (8)a for C_0=0.1 and 0.2 mg/cm³ and from Eq. (10) for C_0=2 mg/cm³.

free aqueous solution diffusivity values, D, reported for each protein by Tyn and Gusek [31] ($6.0\cdot10^{-7}$, $7.8\cdot10^{-7}$, and $10.6\cdot10^{-7}$ cm²/s for BSA, ovalbumin, and α-lactalbumin respectively).

As is seen in Fig. 5, the same diffusivity value provides an excellent fit of the BSA data for both Q-HyperD-F and Q-HyperD-M when the initial protein concentration is 2.0 mg/cm³. For these conditions, intraparticle mass transfer is controlling and the rate of fractional approach to saturation, $F=\bar{q}/q_0$, varies inversely with the square of the particle size (see Eq. (9)). A constant effective diffusivity confirms that the different size particles have the same structure and properties. Conversely, when the initial concentration is 0.1 mg/cm³, a different external mass transfer coefficient is found for each Q-HyperD grade, consistent with the fact that for fine particles suspended in agitated contactors lower mass transfer coefficients are normally found as the particle size is increased [32]. For both low and high protein concentrations the fit is quite good, although some more significant deviations occur at short times when the high concentration runs are fitted neglecting the external film resistance. This is expected, however, since for very short times when the particles are almost completely devoid of protein, the external film resistance should be important even when the protein concentration in solution is very high. Data for ovalbumin and α-lactalbumin were obtained only with Q-HyperD-M. Higher intraparticle diffusivities and external film coefficients are found for these smaller proteins compared with BSA.

Table 2
Kinetic parameters for adsorption on Q-HyperD media in a 50 m*M* Tris–HCl buffer at pH 8.6

Protein	Media	D_s (cm²/s)	k_f (cm/s)	$Sh=k_f d_p/D$
BSA	Q-HyperD-F	$9.2\cdot10^{-9}$	$2.5\cdot10^{-3}$	20.4
BSA	Q-HyperD-M	$9.2\cdot10^{-9}$	$1.4\cdot10^{-3}$	17.7
OVA	Q-HyperD-M	$15\cdot10^{-9}$	$1.9\cdot10^{-3}$	18.5
LACT	Q-HyperD-M	$16\cdot10^{-9}$	$2.5\cdot10^{-3}$	17.9

To confirm the validity of these determinations of mass transfer parameters, we also carried out experiments at intermediate protein concentrations and compared these runs with the predictions of the full model including both external and intraparticle resistances. The results are shown in Fig. 7 and Fig. 8. The model equations (Eqs. (4–6)) were solved numerically using a procedure similar to that described by Saunders et al. [33]. In this procedure, the particle conservation equation (Eq. (4)) is discretized in the radial direction by orthogonal collocation using Jacobi polynomials. The resulting system of ordinary differential equations is then integrated numerically along with the fluid phase mass balance (Eq. (5)) using IMSL routine DVIPAG. The mass action law isotherm was used in carrying out these calculations. Eq. (6) was solved using the Newton's method to find the interfacial composition at each time step in the integration routine. The equilibrium parameters, q_n, n, and K used in the simulations were those obtained from the static equilibrium experiments. The mass transfer parameters, k_f and D_s, were those given in Table 2, which were determined by matching the limiting solutions of the model for

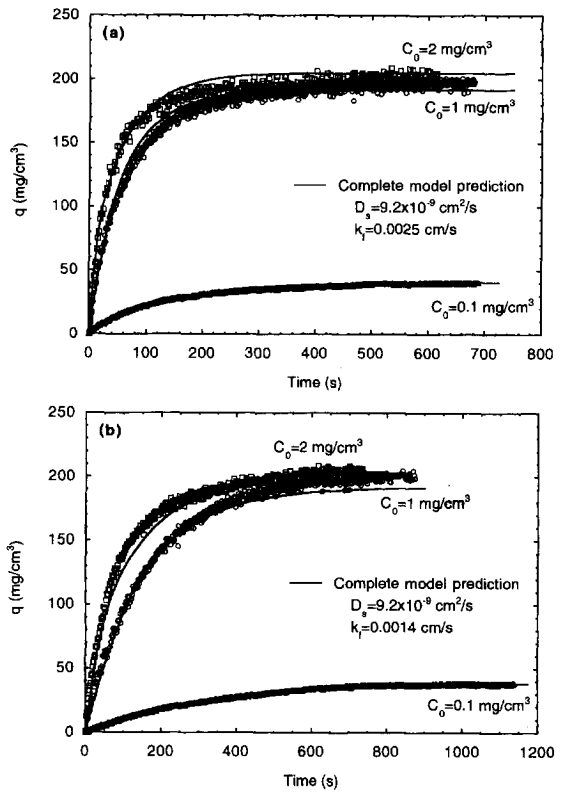

Fig. 7. Transient uptake of BSA by (a) Q-HyperD-F and (b) Q-HyperD-M for different initial protein concentrations in a 50 m*M* Tris–HCl buffer at pH 8.6, Lines are obtained from the numerical solution of the complete kinetic model including both external and intraparticle resistances (Eqs. (4–6)) using the parameters in Tables 1 and 2.

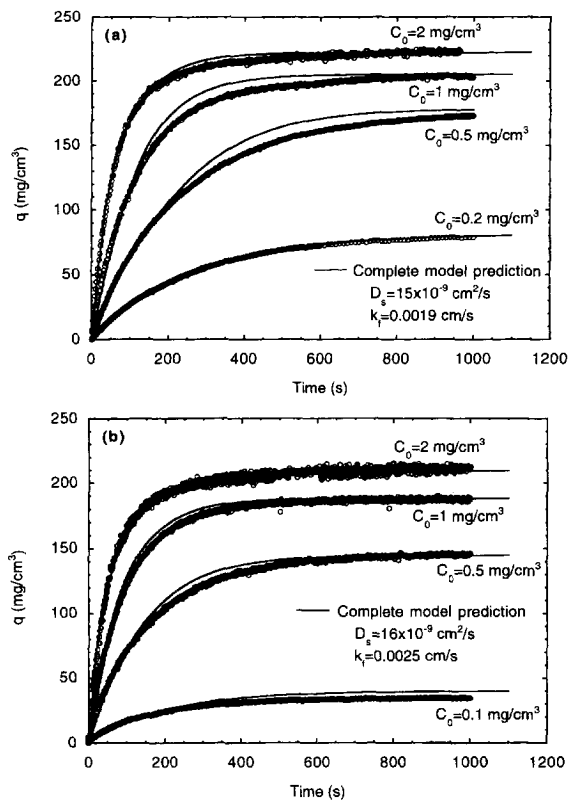

Fig. 8. Transient uptake of (a) ovalbumin and (b) α-lactalbumin by Q-HyperD-M for different initial protein concentrations in a 50 m*M* Tris–HCl buffer at pH 8.6. Lines are obtained from the numerical solution of the complete kinetic model including both external and intraparticle resistances (Eqs. (4–6)) using the parameters in Tables 1 and 2.

external and intraparticle mass transfer control to the low and high concentration data. These parameters are, in principle, independent of concentration. Thus, if the model is correctly formulated, they should provide a good prediction of data at any intermediate protein concentration. This is indeed observed as shown in Fig. 7 and Fig. 8. In each case, at low concentration there is essentially no difference between the numerical solution of the full kinetic model and the analytical solution for external film mass transfer control, confirming that intraparticle mass transfer limitations are indeed absent for these conditions. Similarly, at high concentration, the numerical solution of the full kinetic model is very close to the analytical solution that takes into account intraparticle mass transfer only, indicating that for these conditions external mass transfer resistance is indeed negligible. It should be noted that the prediction of the high concentration uptake curves is actually significantly better with the full kinetic model than with the solution for intraparticle mass transfer only, since the former correctly predicts finite mass transfer rates for short times while the latter incorrectly predicts an infinite rate of mass transfer at the initial time. At each intermediate protein concentration both external film resistance and intraparticle mass transfer resistance are important, but, of course, both D_s and k_f should remain

approximately the same. As shown in Figs. 7 and 8, the effects of both of these resistance combined are accurately predicted by the full kinetic model, demonstrating the validity of the experimentally determined values of D_s and k_f for each protein.

A second test of the validity of the external film mass transfer coefficients obtained experimentally consists of comparing the calculated Sherwood number with values that can be obtained with literature correlations. Armenante and Kirwan [34] have carried out a very extensive investigation of mass transfer to fine particles suspended in an agitated contactor. Their data include broad ranges of particle sizes (6–427 μm) and Schmidt numbers (Sc = 420–130 000) covering the range of particle sizes and Schmidt numbers pertaining to our experiments with Q-HyperD. Armenante and Kirwan have suggested the following empirical correlation to predict the Sherwood number in agitated contactors

$$Sh = 2 + 0.52\left(\frac{\bar{\epsilon}^{1/3} d_p^{4/3}}{\nu}\right)^{0.52} Sc^{1/3} \qquad (11)$$

where $\bar{\epsilon}$ is the mixer power input per unit mass of fluid, d_p is the particle diameter, ν is the kinematic viscosity, and $Sc = \nu/D$ is the Schmidt number. This correlation is plotted in Fig. 9 along with data from several other investigators that have been summarized by Armenante and Kirwan (see Fig. 11 in [34] for the key to the experimental points in this graph). Following Armenante and Kirwan, the power input is estimated from power number correlations as a function of the agitation speed and the geometry of the stirrer with the methods of Uhl and Grey [35]. Such an estimation can, of course, be somewhat inaccurate. However, since the power of $\bar{\epsilon}$ in Eq. (11) is quite small, even relatively large errors in $\bar{\epsilon}$ lead to relatively small errors in the estimated mass transfer coefficient. Moreover, at high agitation speeds, power number correlations typically approach a constant power number, which improves the accuracy of estimation of $\bar{\epsilon}$.

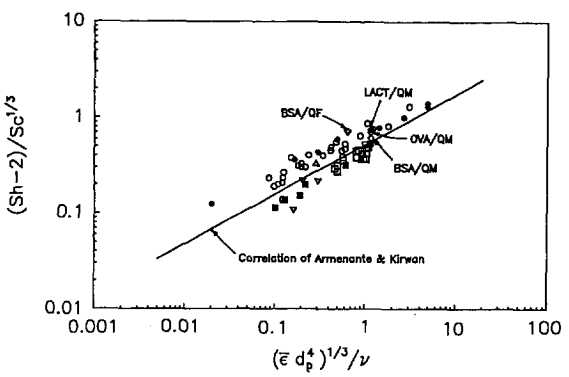

Fig. 9. Comparison of experimental Sherwood number obtained in this work for Q-HyperD media (F and M grades) with literature data for other systems summarized by Armenante and Kirwan [34]. Literature data are represented by the same symbols as Fig. 11 in [34]. Data obtained in this work are labeled individually.

Using the methods of Uhl and Grey [35] for our system, which comprises a 4-cm impeller at 300 rpm with 100 cm^3 of solution, we have estimated a power input $\bar{\epsilon} = 450 \pm 190$ cm^2/s^3. Our data for Q-HyperD-F and M are plotted in Fig. 9, using this estimated value of $\bar{\epsilon}$. As seen in this figure, there appears to be substantial agreement between our experimental mass transfer coefficients for proteins to Q-HyperD particles with the data of several other investigators for different systems and with the correlation of Armenante and Kirwan.

Finally, we have also considered explicitly the effect of the particle size distribution on modeling uptake rates. In fitting the experimental data with Eq. (9) or Eq. (10), we used the volume-average particle radius of each media sample. It is well known (see, for example, [36]) that use of the volume-average size is generally satisfactory provided that the particle size distribution is reasonably symmetrical. We verified that such an approximation is valid for HyperD by solving the model equations numerically while taking into account the particle size distribution in an explicit manner. Using Q-HyperD-M as a test case, we assumed that this media comprises particles with nine different sizes following the particle size distribution of Fig. 1b. The particles are assumed to be identical otherwise. The conservation equations were then solved numerically for each particle size using the fluid phase mass balance to account for the change in solution concentration. We found that the results of these numerical simulations were essentially coincident with those obtained using the volume-average particle radius indicating that the

particle size distribution of HyperD permits the use of the volume-average radius to perform mass transfer calculations.

4. Discussion and conclusions

We have obtained uptake equilibria and mass transfer rates in an a batch contactor for representative proteins with Q-HyperD media. These chromatographic stationary phases, comprising composite porous silica–polyacrylamide gel particles, possess an extremely large static sorption capacity for proteins. The uptake is reversible, and proteins can be effectively desorbed by increasing the salt concentration in the aqueous buffer. The uptake equilibria are represented accurately by the mass action law model, which allows a prediction of isotherms at different counterion concentration with only three parameters. Mass transfer rates in batch experiments in which the Q-HyperD media were suspended in an agitated protein solution were found to be strongly dependent on the solution concentration. At high protein concentrations, mass transfer rates are dominated by intraparticle diffusional limitations. Conversely, at low protein concentrations, mass transfer rates are limited by the external film mass transfer resistance. Kinetic parameters for these two mechanisms could thus be determined independently by carrying out experiments at low and high protein concentrations. This behavior is consistent with an intraparticle mass transfer mechanism in which the sorbed protein concentration provides the driving force for diffusion. Since the sorption capacity of Q-HyperD is quite high, the sorption kinetics is very rapid, even if the gel diffusivities are small in comparison with free-solution diffusivities. As a consequence, a nearly complete saturation of the HyperD media is obtained in as little as 5–10 min with a protein solution concentration of 2 mg/cm^3.

Although the pseudo-homogeneous diffusion model expressed by Eqs. (4–6) provides an excellent fit of the data at high protein concentrations and is capable of predicting the data at intermediate concentrations, one might wonder if other models could provide an equally good or better fit. A key assumption underlying Eqs. (4–6), is that intraparticle transport occurs through the diffusion of "sorbed" protein molecules which interact electrostatically with the ion-exchange functionality of the sorbent particles. The counterpart to this model is one where only "free" or "unbound" protein is allowed to diffuse within the stationary phase. The driving force for diffusion, in this case, is provided by the free protein concentration, which, of course, cannot exceed the external solution concentration. Since the sorption of proteins by Q-HyperD is extremely favorable at low salt concentrations, diffusion of unbound protein would be very well approximated by the well known "shrinking core model". In this model, it is assumed that at each time within a particle there exists an inner core completely devoid of protein surrounded by a fully saturated shell. All of the protein binding takes place irreversibly at the core–shell boundary, which advances toward the center of the particle during the course of the adsorption process. According to this model, the fractional approach to saturation, $F=\bar{q}/q_0$, in a batch system with a finite volume can be derived as shown by McKay [37]. The following expression is obtained

$$\frac{D_e C_0}{R_p^2 q_0} t = \frac{1}{6\Lambda a}\left\{2\sqrt{3}\left[\tan^{-1}\frac{2-a}{a\sqrt{3}} - \tan^{-1}\frac{2\xi-a}{a\sqrt{3}}\right] + \ln\left[\frac{(\xi+a)^2(1-a+a^2)}{(1+a)^2(\xi^2-\xi a+a^2)}\right]\right\} + \frac{1}{3\Lambda}\ln\left[\frac{\xi^3+a^3}{1+a^3}\right] \quad (12)$$

where

$$\xi = \left(1-\frac{\bar{q}}{q_0}\right)^{\frac{1}{3}} \quad (12a)$$

$$\Lambda = \frac{V_M q_0}{V C_0} \quad (12b)$$

$$a = \left(\frac{1-\Lambda}{\Lambda}\right)^{\frac{1}{3}} \quad (12c)$$

In these equations, D_e is the effective diffusivity of the unbound protein in the stationary phase.

A plot of this equation for conditions similar to

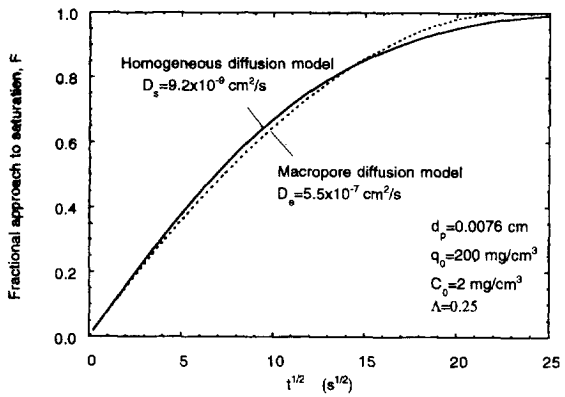

Fig. 10. Comparison of the predictions of the particle diffusion model (Eq. (10)) with $D_s = 9.2 \cdot 10^{-9}$ cm^2/s and the shrinking core model (Eq. (12)) with $D_e = 5.5 \cdot 10^{-7}$ cm^2/s for the transient uptake of BSA by Q-HyperD-M under conditions of intraparticle mass transfer control. The same adsorption capacity, $q_0 = 200$ mg/cm^3 is used in both models.

those used in our batch uptake experiments with Q-HyperD-M with a protein concentration of 2 mg/cm^3 of BSA is given in Fig. 10. The graph also gives the profile calculated from the pseudo-homogeneous diffusion model (Eq. (9) or Eq. (10)) which provided an excellent fit of the experimental data with $D_s = 9.2 \cdot 10^{-9}$ cm^2/s. From this figure, it is apparent that an approximate fit of the same experimental data could be obtained with the shrinking core model. However, that model would require an effective diffusivity D_e in the order of $5.5 \cdot 10^{-7}$ cm^2/s.

The effective diffusivity, D_e, is related to the free aqueous solution diffusivity of the protein, D, by the equation

$$D_e = \frac{\epsilon_p D}{\tau} \lambda \qquad (13)$$

where ϵ_p is the particle porosity, τ the particle tortuosity factor, and λ is a hindrance parameter [9]. Values of τ for typical porous particles range between 2 and 6 [38]. The hindrance parameter varies, of course, with the size of the diffusing solute. However, even for pores that contain no gel and which are simply filled with liquid, λ, representing the ratio of the pore and free diffusivities, is always less than one. Of course, even lower values of the hindrance parameter could be expected for diffusion within pores that are filled with polyacrylamide gel, as in the HyperD media. Park et al. [39], for example, have studied the diffusion of non-interacting molecules in polyacrylamide gels by holographic relaxation methods. They found that the diffusivity of BSA labeled with *p*-(isothiocyano)azobenzene in hydrogels with polymer concentrations as low as 0.025 g/cm^3 was only about 50% of the free solution diffusivity. In more concentrated hydrogels, containing up to 0.134 g/cm^3 of polymer, the labeled BSA diffusivity was reduced to only about 2% of the free diffusivity. If we assume that the entire porosity of the support particles used to prepare the HyperD media (~0.65) is available for diffusion, the free diffusivity that would be consistent with the fitted D_e value would have to be substantially greater than about $1.7 \cdot 10^{-6}$ cm^2/s. Such a value, however, is about three times larger than the actual solution diffusivity of BSA! Even greater values, of course, would be required if diffusion were assumed to occur only over a fraction of the support porosity. Thus, it is apparent that the shrinking core model is completely unable to describe the transient uptake behavior of BSA with a physically realistic value of the effective diffusivity. Therefore, it cannot be considered as a mechanistically valid model. On the other hand, from a phenomenological viewpoint, it is quite clear that diffusion of electrostatically interacting protein in the hydrogel that fills the pores of the HyperD media is the principal mechanism of intraparticle mass transfer. This chromatography medium owes its rapid uptake kinetics to its high sorption capacity which provides a large driving force for diffusion. In Part II of this paper we address mass transfer rates in columns packed with Q-HyperD media and relate the equilibrium and mass transfer parameters to chromatographic performance.

5. Symbols

b	Langmuir isotherm parameter, Eq. (2)
C	protein concentration in solution
C_i	concentration at particle–fluid interface
C_I	counterion concentration
C_0	initial protein concentration

d_p particle diameter
D free solution diffusivity
D_e effective diffusivity in adsorbent particle
D_s diffusivity in adsorbent particle
F fractional approach to saturation
K mass action law parameter, Eq. (3)
k_f film mass transfer coefficient
n effective charge of protein
q protein concentration in adsorbent based on particle volume
q_i adsorbate concentration at particle–fluid interface
q_m Langmuir isotherm parameter, Eq. (2)
q_n mass action law parameter, Eq. (3)
q_R total ion concentration in adsorbent particle
q_0 adsorption capacity based on particle volume
$\bar{q}$ average protein concentration in adsorbent based on particle volume
r radial coordinate in particle
R_p particle radius
Sc Schmidt number (ν/D)
Sh Sherwood number ($=d_p k_f/D$)
t time
V solution volume
V_M adsorbent volume
δ parameter defined by Eq. (7)
τ tortuosity factor
ϵ_p particle porosity
$\bar{\epsilon}$ power input per unit mass of fluid
ν kinematic viscosity
λ diffusional hindrance parameter

Acknowledgments

This research was supported in part by BioSepra, Inc. M.A.F. is grateful for the support by FIYCT of Asturias, Spain. G.C. is indebted to S. Kessler for insightful discussions.

References

[1] Cs. Horvath and S.R. Lipsky, J. Chromatogr. Sci., 7 (1969) 109.
[2] K. Kalghatgi and Cs. Horvath, J. Chromatogr., 398 (1987) 335.
[3] J.V. Dawkins, L.L. Lloyd and F.P. Warner, J. Chromatogr., 352 (1986) 157.
[4] L.L. Lloyd and F.P. Warner, J. Chromatogr., 512 (1990) 365.
[5] N.B. Afeyan, N.F. Gordon, I. Mazsaroff, L. Varady, S.P. Fulton, Y.B. Yang and F.E. Regnier, J. Chromatogr., 519 (1990) 1.
[6] A.E. Rodrigues, Z.P. Lu and J.M. Loureiro, Chem. Eng. Sci., 107 (1991) 2765.
[7] G. Carta, M. Gregory, D.J. Kirwan and H. Massaldi, Sep. Technol., 2 (1992) 273.
[8] A.I. Liapis and M.A. McCoy, J. Chromatogr., 599 (1992) 87.
[9] D. Frei, E. Schweinheim and Cs. Horvath, Biotechnol. Prog., 9 (1993) 273.
[10] E. Boschetti, J. Chromatogr. A, 658 (1994) 207.
[11] J.L. Tayot, M. Tardy, P. Gattel, R. Plan and M. Roumiantzeff, in R. Epton (Editor), Chromatography of Synthetic and Biological Polymers, Ellis Horwood, Chichester, 1978, p. 95.
[12] M.G. Bite, S. Berezenko and F.J.S. Reed, in M. Streat (Editor) Ion Exchange for Industry, Ellis Horwood, Chichester, 1988, p. 193.
[13] D. Mislovicova, M. Petro and D. Berek, J. Chromatogr., 646 (1993) 411.
[14] J. Horvath, E. Boschetti, L. Guerrier and N. Cooke, J. Chromatogr. A, 679 (1994) 11.
[15] A. Jungbauer, H.P. Lettner, L. Guerrier and E. Boschetti, BioPharm, July–August 1994, p. 37.
[16] P. Girot and E. Boschetti, US Pat., 5 258 097 (1993).
[17] S.B. Kessler, personal communication, 1994.
[18] Q-HyperD F/M, Material safety data sheet, 1993.
[19] D.S. Grzegorczyk and G. Carta, Chem. Eng. Sci., 51 (1996) 819.
[20] A. Velayudhan and Cs. Horvath, J. Chromatogr., 443 (1988) 13.
[21] H.-S. Tsou and E.E. Graham, AIChE J., 31 (1985) 1959.
[22] G.L. Skidmore, B.J. Horstmann and H.A. Chase, J. Chromatogr., 498 (1990) 113.
[23] G.F. Bloomingburg and G. Carta, Chem. Eng. J., 55 (1994) B19.
[24] F.E. Regnier and I. Maszaroff, Biotechnol. Prog., 3 (1987) 22.
[25] R.D. Whitley, R. Wachter, F. Liu and N.-H.L. Wang, J. Chromatogr., 465 (1989) 137.
[26] C.A. Brooks and S.M. Cramer, AIChE J., 38 (1992) 1969.
[27] E.E. Graham, A. Pucciani and N.G. Pinto, Biotechnol. Prog., 3 (1987) 141.
[28] H. Yoshida, M. Yoshikawa and T. Kataoka, AIChE J., 40 (1994) 2034.
[29] F. Helfferich, Ion Exchange, McGraw-Hill, New York, 1962, pp. 255–260.
[30] F. Helfferich and M.S. Plesset, J. Chem. Phys., 28 (1958) 418.
[31] M.T. Tyn and T.W. Gusek, Biotechnol. Bioeng., 35 (1990) 327.
[32] S. Asai, Y. Konishi and Y. Sasaki, J. Chem. Eng. Jpn., 21 (1988) 107.
[33] M.S. Saunders, J.B. Vierow and G. Carta, AIChE J., 35 (1989) 53.

[34] P.M. Armenante and D.J. Kirwan, Chem. Eng. Sci., 44 (1989) 2781.
[35] V.W. Uhl and J.B. Grey (Editors), Mixing: Theory and Practice, Vol. 1, Academic Press, New York, 1966, pp. 111–172.
[36] G. Carta and J.S. Bauer, AIChE J., 36 (1990) 147.
[37] G. McKay, Chem. Eng. Res. Dev., 62 (1984) 235.
[38] D.M. Ruthven, Principles of Adsorption and Adsorption Processes, Wiley, New York, 1984, p. 134.
[39] H.H. Park, C.S. Johnson, Jr. and D.A. Gabriel, Macromolecules, 23 (1990) 1548.